Taylor & Francis
Taylor & Francis Group

ORIGINAL RESEARCH ARTICLE

🔓 OPEN ACCESS Check for updates

Circulating exosome microRNA associated with heart failure secondary to myxomatous mitral valve disease in a naturally occurring canine model

Vicky K. Yang, Kerry A. Loughran, Dawn M. Meola, Christine M. Juhr, Kristen E. Thane, Airiel M. Davis and Andrew M. Hoffman

Department of Clinics Sciences, Tufts University Cummings School of Veterinary Medicine, North Grafton, USA

ABSTRACT

Myxomatous mitral valve disease (MMVD) is functionally and histologically identical to mitral valve prolapse (MVP) in humans. Currently, there are no medical treatments that can delay the progression of this valvular disease or associated cardiac remodelling. Therefore, there is a need to understand the molecular pathology associated with MMVD and MVP better, and thus identify potential therapeutic targets. Circulating exosomes contain small RNA, including miRNA, which reflect cell physiology and pathology. This study explored the association between circulating exosomal miRNA (ex-miRNA) content and MMVD, heart failure due to MMVD (MMVD-CHF) and ageing, which is strongly associated with MMVD. Ex-miRNA was isolated from old normal/healthy dogs ($n = 6$), young normal dogs ($n = 7$), dogs with MMVD ($n = 7$) and dogs with MMVD-CHF ($n = 7$). Separately, total plasma miRNA was isolated from normal dogs ($n = 8$), dogs with MMVD ($n = 8$) and dogs with MMVD-CHF ($n = 11$). Using reverse transcription quantitative polymerase chain reaction, exosomal miR-181c ($p = 0.003$) and miR-495 ($p = 0.0001$) significantly increased in dogs with MMVD-CHF compared to the other three groups. Exosomal miR-9 ($p = 0.002$) increased in dogs with MMVD and MMVD-CHF compared to age-matched (old) normal dogs. Exosomal miR-599 ($p = 0.002$) decreased in dogs with MMVD compared to old normal dogs. In total plasma, 58 miRNA were deemed significantly different ($p < 0.04$) between normal dogs, dogs with MMVD and dogs with MMVD-CHF. However, in contrast to ex-miRNA, none of the miRNA in total plasma remained statistically significant if the false discovery rate was <15%. Changes in ex-miRNA are observed in dogs as they age (miR-9, miR-495 and miR-599), develop MMVD (miR-9 and miR-599) and progress from MMVD to CHF (miR-181c and miR-495). Ex-miRNA expression-level changes appear to be more specific to disease states than total plasma miRNA.

Introduction

Mitral valve prolapse (MVP) is a common valvular heart disease, with a prevalence of 3% in the adult population. Histological changes include disruption and fragmentation of the collagen and elastin fibres within the valves. These abnormalities are often referred to as myxomatous changes [1]. Although most MVP events are benign, ruptured chordae or poor coaptation of the valve leaflets can lead to mitral regurgitation (MR) with ensuing congestive heart failure (CHF). Currently, medical management of MR is of limited value, and mitral valve repair or replacement are most effective when provided before the onset of CHF [2]. The mortality rate with surgery ranges from 2% to 6% and is twice as high for the elderly, and 7–10% of patients require reoperation within 10 years [2]. Given the high rate of mortality for the elderly and those already in CHF, there is a strong rationale to develop novel medical interventions that will mitigate progression

of MVP or slow the deterioration of cardiac function. The process of exploring molecular targets for MVP would be greatly aided by the use of an appropriate animal model. Naturally occurring myxomatous mitral valve disease (MMVD) in dogs closely resembles MVP in humans with respect to structural and functional consequences, making this canine disease an attractive preclinical model for human therapies. MMVD is the most common acquired cardiac disease and the most common cause of CHF in dogs, comprising two-thirds of all canine cardiac cases [3]. This disease is age related, and its prevalence in older small-breed dogs reaches 100% [3]. MMVD leads to MR, cardiac enlargement and contractile dysfunction in the later stages. Once in CHF, dogs are reported to have a median survival time between 1 and 9 months [3].

Dysregulation of miRNA is often associated with human diseases [4]. In veterinary patients, changes in various miRNA concentrations have been observed in

---

canine ventricular and atrial muscles after CHF development subsequent to experimental ventricular pacing, including the downregulation of cfa-miR-1, cfa-miR-26a, cfa-miR-26b, cfa-miR-29a, cfa-miR-30a, cfa-miR-133a, cfa- miR-133b, cfa-miR-208a and cfa-miR-218, and the upregulation of cfa-miR-21 and cfa-miR-146b [5]. In addition, cfa-miR-206 expression is increased with atrial fibrillation induced by right atrial tachypacing in dogs [6]. In canine MMVD, Li et al. have shown the downregulation of serum cfa-miR-302d, cfa-miR-380, cfa-miR-874, cfa-miR-582, cfa-miR-490, cfa-miR-329b and cfa-miR-487b, and the upregulation of cfa-miR-103, cfa-miR-98, cfa-let-7b and cfa-let-7c [7]. Similarly, analysis of plasma miRNA in Dachshunds with MMVD has shown a downregulation of known cardioprotective miRNA (cfa-miR-30b and cfa-miR-133b) [8].

These studies, however, neither address miRNA expression in diseased tissues of dogs with naturally occurring MMVD, nor attempt to relate circulating miRNA with diseased tissues and pathophysiology. One approach to understand the role of miRNA better that arise from diseased tissues or immune cells is the analysis of circulating exosomal miRNA (ex-miRNA) signatures. Exosomes are nanoscale vesicles ranging in size from 40 to 120 nm [9]. The miRNA content of exosomes is highly regulated by the cell of origin, and depends on the physiological and pathological molecular signals at work during the time of exosome production [10]. It was hypothesised that exosome miRNA will discriminate healthy, MMVD and/or MMVD-CHF, and will do so more efficiently than total plasma analysis of miRNA. This study did not hypothesise the cellular origin of exosome miRNA.

The first goal of this study was to identify changes in circulating ex-miRNA expression levels in dogs with MMVD or MMVD with CHF compared to normal, healthy control dogs with no cardiac disease. It also examined the effect of age in control dogs, as MMVD is strongly age related. The second goal was to understand the range of miRNA isolated from ex-miRNA compared to unfractionated (total) plasma miRNA to see if ex-miRNA are more disease relevant. It was hypothesised that analysis of ex-miRNA in MMVD would lead to candidate miRNA with in silico targets that are associated with disease pathogenesis, suggesting ex-miRNA offer a unique strategy to study the biology and natural history of MMVD.

Methods

Animals

The study protocol was reviewed and approved by the Tufts University Cummings School of Veterinary Medicine Clinical Studies Review Committee. A total of 47 client-owned dogs were enrolled under consent by their owners. Each dog received a physical examination and an echocardiographic evaluation. Dogs with observed or history of respiratory signs also received chest radiographs. The dogs were then divided into three groups based on radiographs and echocardiogram: normal healthy dogs, dogs with asymptomatic MMVD and dogs with MMVD and history of CHF (MMVD-CHF). Diagnosis and classification of MMVD followed the guidelines published by the American College of Veterinary Internal Medicine Consensus Statement for canine mitral valve disease [11]. The MMVD group consisted of dogs with MR and thickening or prolapsing of the mitral valve leaflets but that did not have clinical signs of heart failure. The MMVD-CHF group consisted of dogs with MMVD and past or current clinical signs for heart failure, where heart failure had been verified with radiographic signs for pulmonary oedema. Echocardiographic findings are described in Supplementary Tables S1 and S2. Dogs with other systemic diseases such as systemic hypertension, uncontrolled hypothyroidism, hyperadrenocortism, primary pulmonary hypertension, neoplasia and other cardiac abnormalities such as dilated cardiomyopathy, congenital cardiac abnormalities, endocarditis and severe arrhythmia were excluded from the study. Whole blood sample were collected from each dog via venipuncture into EDTA tubes (BD Biosciences).

Total plasma miRNA isolation

Plasma was isolated by centrifuging the whole blood sample at 1,320 g for 10 min at room temperature immediately after blood collection to remove cells and platelets. Plasma was stored at –80°C until the time of processing. After thawing, miRNA were extracted from 0.4 mL of plasma using Trizol LS (Thermo Fisher Scientific). Total miRNA was then isolated using the a miRNeasy kit (Qiagen) according to the manufacturer's instructions.

Plasma ex-miRNA isolation

Plasma samples were prepared as above. Exosomes from 1 mL of plasma were isolated using sequential centrifugation (2,000 g for 10 min and 10,000 g for 30 min, both at room temperature) followed by a final ultracentrifugation step (100,000 g for 2 h at 4°C) [12]. Western blot showed that the exosome pellets isolated from the ultracentrifugation steps did not contain high levels of Argonaute2 (see Supplementary Figure S1). In addition, the ultracentrifuged pellets contained TSG101 based on enzyme-linked

immunsorbent assay (ELISA; 2.1 ng/mL, STD 1.4, $n = 3$; Canine Tumor Susceptibility Gene 101 ELISA Kit, Mybiosource.com, cat # MBS077995) and are therefore enriched with exosomes. Ex-miRNA was then isolated by resuspending the pellet in phosphate-buffered saline (PBS; 1 mL) and applying to a spin column (ExoRNeasy kit; Qiagen). Using this isolation method, it was observed that treating the exosomes with 2 mg/mL of proteinase K (Qiagen) and 2 mg/mL of RNase A (Qiagen) had no significant effect on the quantity of selected ex-miRNA, suggesting that samples contained minimal or no non-exosomal miRNA (see Supplementary Figure S2). It was also observed that the isolation process using the spin column resulted in minimal amount of liproprotein contamination (see Supplementary Figure S3).

Characterisation of exosomes isolated from plasma

Exosomes from representative samples were immunolabelled for bead-assisted flow cytometry to evaluate CD9 expression [13]. Briefly, immunolabelling was performed by absorbing isolated exosomes onto 4 μm latex beads (Thermo Fisher Scientific) with overnight incubation at room temperature. The exosome-coated beads were incubated (1 h at room temperature) with canine-reactive mouse monoclonal biotinylated anti-CD9 antibody (Abcam) or mouse IgG$_{2b}$ biotinylated isotype antibody (Abcam), and then streptavidin-PE (30 min at room temperature) as the secondary antibody. Exosome size distribution and concentration were evaluated with both transmission electron microscopy (TEM) using uranium acetate negative staining and nanoparticle tracking analysis (NTA; NS300, software v3.0; Malvern). Samples for NTA were diluted in sterile, commercially available PBS to achieve a working concentration of $1–10 \times 10^8$ particles/mL. Specific NTA settings include laser wavelength (488 nm), temperature (23°C), screen gain (1.0), camera level (13) and infusion pump (5 μL/min). Five videos were recorded per sample, with 30–60 s per video, a minimum of 200 valid tracks per video and a minimum of 1,000 valid tracks per sample. The detection threshold was set at 5 with auto blur and auto max jump distance settings. Validation of size accuracy was periodically performed using polystyrene beads of known size (100 and 200 nm).

Reverse transcription quantitative polymerase chain reaction

cDNA was synthesised using a miScript II RT kit (Qiagen) according to the manufacturer's instructions. Pre-amplification was performed using miScript PreAmp PCR kit (Qiagen). Reverse transcription quantitative polymerase chain reaction (RT-qPCR) was performed using Canine miRNome miScript miRNA PCR Array (Qiagen), an array based on canine-specific sequences in miRBase v16, for the detection of 277 canine miRNA. A total of 40 cycles of amplification were performed with RT-qPCR. C_q values within each sample were normalised using the geomean of all detected miRNA in that sample [14,15]. Undetected miRNA were assigned a C_q number of 40 prior to normalisation.

Statistical and data analysis

Statistical analysis was performed using the Kruskal–Wallis test for comparison of more than two groups, and the Mann–Whitney U-test for two-way comparisons. Further analysis was completed using the Benjamini–Hochberg procedure [16], with a false discovery rate (FDR) of 20%. Targets were predicted in silico using a combination of TargetScan [17] and miRDB [18]. Only targets predicted by both programmes were used in the interaction network analysis. Hierarchical clustering (HCL) was performed using Multiexperimental Viewer (MeV 4.9.0) [19].

Results

Total plasma miRNA

Demographic profile

A total of 27 dogs were enrolled in this part of the study. Dogs were divided into three groups: normal dogs with no age limitation ($n = 8$), dogs with asymptomatic MMVD ($n = 8$) and dogs with MMVD and a history of CHF ($n = 11$). The demographic profiles are shown in Table 1. The normal group was significantly younger ($p = 0.001$) than the other two groups. Dogs in the MMVD-CHF group had lower body weights than the normal dogs ($p = 0.003$). However, there was no significant difference in age or weight between the dogs in the MMVD and MMVD-CHF groups.

Hierarchical clustering does not show grouping by disease status

The HCL heat map of total plasma miRNA expression levels based on normalised C_q numbers is shown in Figure 1, with green indicating a higher expression level and red indicating a lower expression level. There was no evidence of miRNA expression clustering by group (normal, MMVD or MMVD-CHF).

MiRNA expression levels differed between disease status

The average number of miRNA detected for each dog was 47% of the 277 miRNA. Of the 277 miRNA, 58 (20.9%) included in the microarray were significantly

Table 1. Total plasma miRNA study dogs.

Disease status	Total	Median age (range), years	Median weight (range), kg	Breed	Total	Gender	Total
Normal	8	3.5 (2–7)	23.5 (10–36)	Beagle	1	CM[‡]	3
				Labrador Retr	1	SF[§]	5
				Gordon Setter	1		
				Pit Bull	2		
				GSP*	1		
				Mixed Breed	2		
MMVD	8	9 (5–13)	7.7 (8–40)	Shih Tzu	1	CM[‡]	3
				CKCS[†]	2	SF[§]	5
				Golden Retr	1		
				Maltese	1		
				Mixed Breed	3		
MMVD with CHF	11	10 (8–13)	7.2 (5–13)	CKCS[†]	3	CM[‡]	4
				Boston Terrier	1	SF[§]	7
				Papillon	1		
				Chihuahua	1		
				Mixed Breed	5		

*GSP = German Shorthair Pointer; †CKCS = Cavalier King Charles Spaniel; ‡CM = castrated male; §SF = spayed female.

different between the three groups using a FDR of 20% (FDR-adjusted p-value of ≤0.042). These miRNA are listed in Table 2. However, when employing a FDR of ≤15%, none of these miRNA remained statistically

Figure 1. Hierarchical clustering heat map for total plasma miRNA. Hierarchical clustering using normalised C_q number for total plasma miRNA expression (green = higher expression, red = lower expression) comparing normal dogs, dogs with myxomatous mitral valve disease (MMVD) and dogs with heart failure due to MMVD (CHF).

significant. When comparing only the MMVD and MMVD-CHF groups using a FDR of 20%, 57 (20.5%) miRNA were significantly different between the two groups (FDR-adjusted p-value of ≤0.039), and when comparing no CHF (i.e. normal dogs and MMVD group) and CHF (i.e. MMVD-CHF group), 78 (28.2%) miRNA were significantly different between the two groups (FDR-adjusted p-value of ≤0.05).
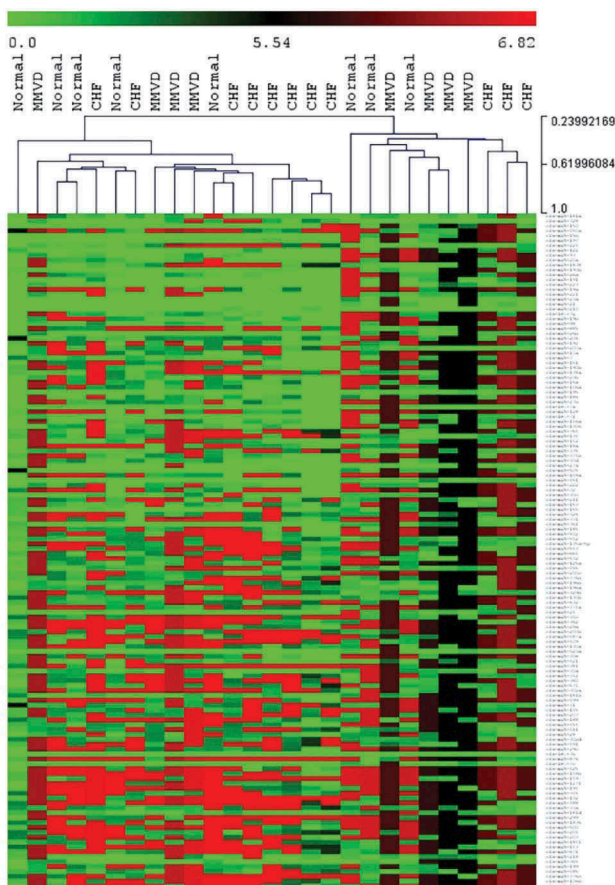
Plasma ex-miRNA

Demographic profile

A total of 27 dogs were enrolled in this part of the study. Dogs were divided into four groups: young normal dogs <7 years old ($n = 6$), old normal dogs ≥7 years old ($n = 7$), dogs with asymptomatic MMVD ($n = 7$), and dogs with MMVD and history of CHF ($n = 7$). Normal dogs were divided into young and old groups for the analysis of ageing effects. Demographic information pertaining to the study dogs is listed in Table 3. There was a statistically significant difference in age between the young normal dogs and the other three groups ($p = 0.001$). There was no difference in weight between the groups.

Characterisation of circulating canine exosomes

As shown by bead-assisted flow cytometry, 99.8% of the exosome-coated latex beads were positive for CD9, suggesting that as a population, circulating exosomes express CD9 (Figure 2(a)), acknowledging the limitation of this technique to establish level of expression. On transmission electron microscopy (TEM) imaging, 82% of the imaged exosomes were between 50 and 70 nm (Figure 2b and c). NTA showed that the majority of the isolated exosomes are between 70 and 100 nm (34.7%; Figure 2c), which is consistent with past observations that TEM preparation shrinks exosomes [20]. A lower-power TEM image is shown in Supplementary Figure S4.

Table 2. List of total plasm miRNAs meeting the 20% FDR criteria using the Benjamini–Hochberg procedure.

Comparison between normal, MMVD and MMVD-CHF groups FDR-adjusted *p*-value ≤0.042 Comparison between MMVD and MMVD-CHF groups FDR-adjusted *p*-value ≤0.039	cfa-let-7a, cfa-miR-105a, cfa-miR-105b, cfa-miR-126, cfa-miR-1271, cfa-miR-129, cfa-miR-1307, cfa-miR-133a, cfa-miR-138b, cfa-miR-139, cfa-miR-142, cfa-miR-149, cfa-miR-181d, cfa-miR-186, cfa-miR-196a, cfa-miR-196b, cfa-miR-200b, cfa-miR-202, cfa-miR-212, cfa-miR-217, cfa-miR-218, cfa-miR-219-5p, cfa-miR-29a, cfa-miR-30b, cfa-miR-325, cfa-miR-329a, cfa-miR-335, cfa-miR-338, cfa-miR-345, cfa-miR-34c, cfa-miR-363, cfa-miR-374b, cfa-miR-376a, cfa-miR-379, cfa-miR-380, cfa-miR-382, cfa-miR-384, cfa-miR-421, cfa-miR-429, cfa-miR-487a, cfa-miR-489, cfa-miR-491, cfa-miR-495, cfa-miR-496, cfa-miR-504, cfa-miR-514, cfa-miR-545, cfa-miR-551a, cfa-miR-568, cfa-miR-578, cfa-miR-592, cfa-miR-708, cfa-miR-759, cfa-miR-761, cfa-miR-764, cfa-miR-802, cfa-miR-872, cfa-miR-99b
	cfa-let-7f, cfa-let-7g, cfa-miR-105a, cfa-miR-105b, cfa-miR-126, cfa-miR-1307, cfa-miR-133a, cfa-miR-139, cfa-miR-141, cfa-miR-142, cfa-miR-149, cfa-miR-181d, cfa-miR-1836, cfa-miR-193a, cfa-miR-196a, cfa-miR-200b, cfa-miR-202, cfa-miR-212, cfa-miR-217, cfa-miR-218, cfa-miR-219-5p, cfa-miR-223, cfa-miR-23a, cfa-miR-29a, cfa-miR-30a, cfa-miR-325, cfa-miR-329a, cfa-miR-338, cfa-miR-363, cfa-miR-367, cfa-miR-374b, cfa-miR-376a, cfa-miR-379, cfa-miR-382, cfa-miR-384, cfa-miR-452, cfa-miR-454, cfa-miR-491, cfa-miR-495, cfa-miR-496, cfa-miR-504, cfa-miR-514, cfa-miR-544, cfa-miR-545, cfa-miR-551a, cfa-miR-568, cfa-miR-578, cfa-miR-592, cfa-miR-652, cfa-miR-665, cfa-miR-708, cfa-miR-759, cfa-miR-761, cfa-miR-802, cfa-miR-872, cfa-miR-876, miR-96

Three group comparison was performed using the Kruskal–Wallis test, and two-way comparisons was performed using the Mann–Whitney *U*-test.
FDR = false discovery rate; MMVD = myxomatous mitral valve disease; MMVD-CHF = heart failure due to MMVD.

Table 3. Plasma ex-miRNA study dogs.

Disease status	Total	Median age (range), years	Median weight (range), kg	Breed	Total	Gender	Total
Young normal group	6	2 (2–4)	10.3 (10–43)	Beagle	3	CM[†]	3
				Mixed Breed	3	SF[‡]	3
Old normal group	7	7.6 (7–10)	6.2 (5–14)	Bichon	1	CM[†]	4
				Corgi	1	SF[‡]	3
				Yorkshire	1		
				Terrier	2		
				Shih Tzu	1		
				Lowchen	1		
				Mixed Breed			
MMVD	7	11 (5–13)	7.2 (6–16)	Shih Tzu	1	CM[†]	3
				CKCS*	2	SF[‡]	4
				Border Collie	1		
				Pekinese	1		
				Maltese	2		
MMVD with CHF	7	10 (6–11)	8.2 (3–14)	CKCS*	2	CM[†]	4
				Boston Terrier	1	SF[‡]	3
				Miniature	1		
				Poodles	3		
				Mixed Breed			

*CKCS = Cavalier King Charles Spaniel; †CM = castrated male; ‡SF = spayed female.

Hierarchical clustering demonstrates striking effect of age on ex-miRNA content

The HCL heat map of ex-miRNA expression levels based on normalised C_q numbers is shown in Figure 3, with green indicating a higher expression level and red indicating a lower expression level. Clustering of dogs from the old normal group was noted in the clustered heat map. The dogs from the young normal group appear to be interspersed with the MMVD and MMVD-CHF groups in the clustered heat map. This may be an indication that certain miRNA may revert back to a "younger" state secondary to effects of MMVD and CHF development (e.g. cardiac remodelling, decreased cardiac output, change in energetics and metabolic state of the heart).

Ex-miRNA patterns reflect the MMVD or MMVD-CHF phenotype

The average number of miRNA detected for each dog was 54% of the 277 miRNA. Out of the 277, four (1.4%) were statistically different between the four groups (FDR-adjusted *p*-value of ≤0.003). These miRNA included cfa-miR-9 ($p = 0.002$), cfa-miR-181c ($p = 0.003$), cfa-miR-495 ($p = 0.0001$) and cfa-miR-599 ($p = 0.002$). In a two-way comparison, cfa-miR-9 was significantly lower in old normal versus young normal dogs (average fold change [FC] = –26.4; $p = 0.006$), dogs with MMVD (FC = –25.8; $p = 0.007$) and dogs with MMVD-CHF (FC = –45.7; $p = 0.0001$). For cfa-miR-181c, there is an increase in expression level for dogs in the MMVD-CHF group compared to young normal
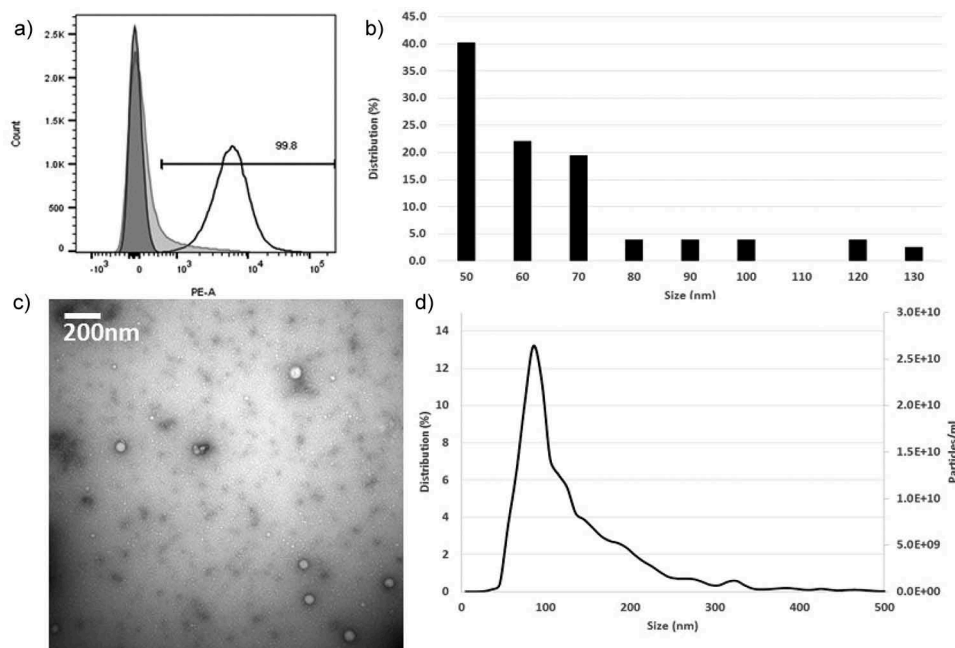
Figure 2. Characterisation of plasma exosomes. (a) Flow cytometry profile of CD9-positive exosomes showing 99.8% of the beads are positive for CD9 (dark grey = latex beads alone, light grey = IgG2b isotype, white = isolated exosomes). (b) Representative transmission electron microscopy (TEM) micrograph of exosomes. (c) TEM size distribution out of a total of 77 exosomes counted. (d) Nanoparticle tracking analysis analysis of microvesicle size distribution.

dogs (FC = 10.7; p = 0.037), old normal dogs (FC = 6.5; p = 0.012) and dogs with MMVD (FC = 23.4; p = 0.0001). For cfa-miR-495, there was an increase in expression for young normal dogs compared to old normal dogs (FC = 6.9; p = 0.004) and dogs with MMVD (FC = 5.8; p = 0.018). There was also an increase in cfa-miR-495 expression in dogs with MMVD-CHF compared to dogs in the old normal (FC = 14.9; p = 0.0001) and MMVD groups (FC = 12.5; p = 0.002). Finally, for cfa-miR-599, there was an increase in expression in old normal compared to young normal dogs (FC = 15.2; p = 0.007) and dogs in the MMVD group (FC = 18.5; p = 0.0001). There was also an increase in expression in dogs with MMVD-CHF compared to dogs in the MMVD group (FC = 3.2; p = 0.02). The changes in expression levels for cfa-miR-9, cfa-miR-181c, cfa-miR-495 and cfa-miR-599 are illustrated in Figure 4 where the normalised C_q values for each of the disease states are shown.

cfa-miR181c and cfa-miR-495 also appear to retain significant differences in expression level when comparing no CHF (i.e. young normal dogs, old normal dogs and MMVD group) and CHF (i.e. MMVD-CHF group; FDR-adjusted p-value of ≤0.001). Compared to dogs without any history of CHF, dogs with CHF have increased expression of cfa-miR-181c (p = 0.00015; FC = 11.8) and cfa-miR-495 (p = 0.001; FC = 7.9).

Ex-miRNA are less prone to false discovery and are more disease relevant than total plasma miRNA

Based on the results, only cfa-miR-495 was significantly different between disease groups in both total plasma and ex-miRNA. However, when comparing between dogs with MMVD and those with MMVD and CHF, cfa-miR-495 decreased in total plasma (p = 0.013; Supplementary Figure S5) but increased in plasma exosomes (Figure 4). Comparing the two studies (using different sets of dogs), there were significantly fewer miRNA out of the 277 analysed showing significant differences between groups in the plasma exosomes compared to total plasma at a FDR of 20%.

Given the large number of total plasma miRNA deemed significantly different between disease groups with a FDR of 20%, the analysis was repeated using FDRs of 5%, 10% and 15%. Looking specifically at the comparison between no CHF (i.e. normal dogs and MMVD group) and CHF (i.e. MMVD-CHF group), the number of miRNA with significant differences in total plasma decreased from 78 to 0 when FDR was decreased from 20% to 10%. On the other
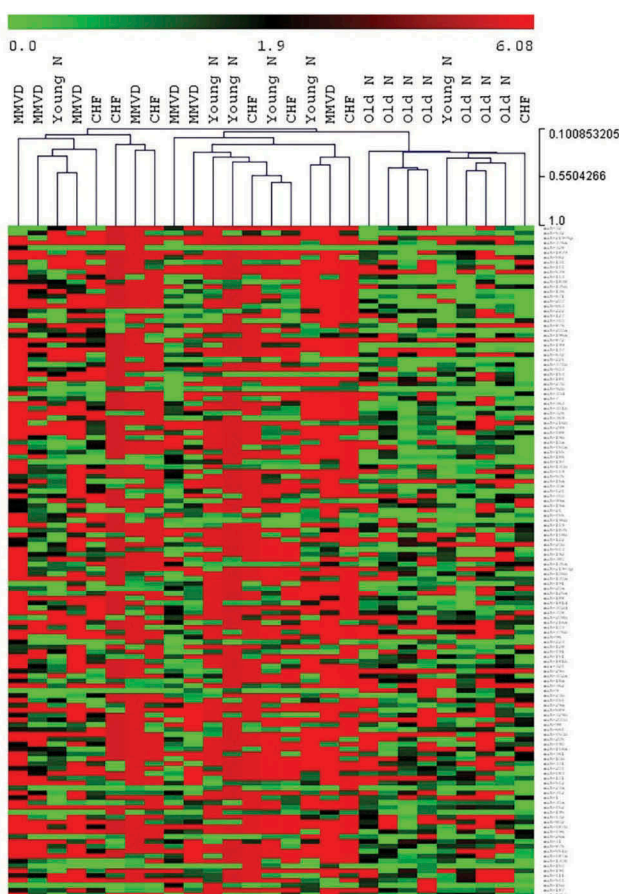
Figure 3. Hierarchical clustering heat map for plasma ex-miRNA. Hierarchical clustering using normalised C_q number for plasma ex-miRNA expression (green = higher expression, red = lower expression) comparing young normal dogs (Young N), old normal dogs (Old N), dogs with MMVD and dogs with MMVD-CHF (CHF).

hand, for the same comparison in ex-miRNA, cfa-miR-181c remained significant at a FDR as low as 5% (Figure 5a), showing that the change in ex-miRNA is a robust finding in this disease model and that there is a high incident of false positives in total plasma miRNA analysis.

To explore this further, the miRNA expression in total plasma and plasma exosome from the same dogs ($n = 8$), including three with MMVD and five with MMVD-CHF, was compared. Out of the 277 miRNA analysed, only nine miRNA had similar expression levels between total plasma and ex-miRNA (<2-fold difference in normalised C_q number). In addition, HCL illustrates closer association in expression levels between miRNA sources rather than by individual dogs (Figure 5b). Particularly, cfa-miR-146a was consistently enriched in plasma exosomes for these eight dogs, with an 86-fold increase in expression level compared to total plasma. These data reinforce that the repertoire of circulating exosomes and total plasma overlap, but the differences substantially alter

the interpretation of data sets. In addition, plasma ex-miRNA content does not reflect that of total plasma, and the two are therefore not interchangeable.

Discussion

The present observations suggest that dysregulation of miR-9 and miR-599 chronologically precedes CHF, suggesting that these miRNA warrant further investigation as putative initiating factors for CHF, while others were found only at the time of CHF (miR-181c and miR-495), which denotes a role in initiation, progression or consequence of CHF. The present data are inconclusive with respect to causality but permit novel hypotheses to be advanced concerning the epigenetic mechanisms of MMVD, left heart enlargement and progression to heart failure.

Plasma exosomal miR-9 expression decreases with age

The data analysis shows that relative to young normal dogs, dogs with MMVD or dogs with MMVD-CHF, the expression level of cfa-miR-9 is low in older normal dogs. MiR-9 has been shown to have anti-fibrotic effects, and overexpression of miR-9 in neonatal rats inhibits the proliferation of cardiac fibroblasts and collagen production [21]. This inhibition is a result of direct targeting and inhibition of PDGFR-β [21]. Both of these effects would suggest that miR-9 has protective effects for cardiac remodelling. Given that MMVD is an age-associated disease affecting almost 100% of older dogs, the pathologic role of declining miR-9 in old normal dogs will need to be investigated further. In addition, longitudinal studies may help us verify if miR-9 content of exosomes rebounds in temporal association with MMVD or CHF.

In contrast, cfa-miR-9 expression once again increases with the development of MMVD, which would suggest that MR, volume-overload, cardiac remodelling or haemodynamic effects on other organs (lungs and kidneys) may initiate or propagate higher expression of circulating cfa-miR-9. However, it is not known if the anti-fibrotic effects of miR-9 are sufficient to counter pro-fibrotic stimuli exerted by volume overload and chronic heart failure. Further studies are needed to test target expression and to verify miR-9 target interactions in diseased tissues to understand these findings.

Plasma exosomal miR-181c is strongly associated with MMVD-CHF

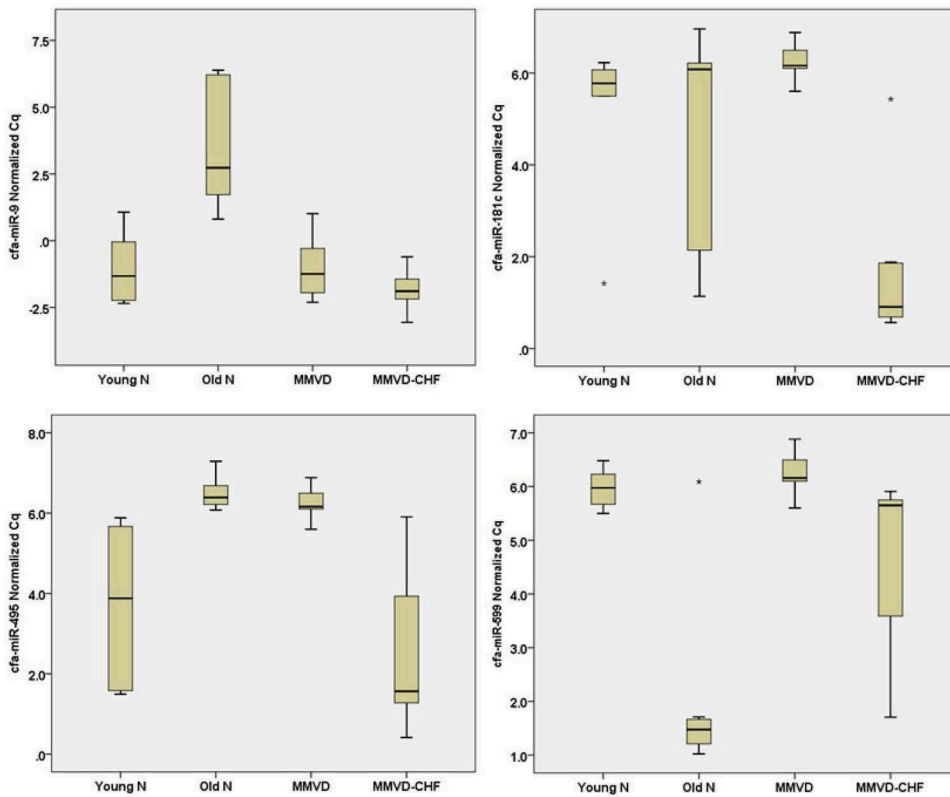The data showed that there is high expression of exosomal cfa-miR-181c in dogs with CHF. MiR-

Figure 4. Expression levels of miR-9, miR-181c, miR-495 and miR-599. Box-plot comparing ex-miRNA expression level as measured with reverse transcription quantitative polymerase chain reaction. A high normalised C_q value indicates low expression level, whereas a low normalised C_q value indicates a high expression level. Asterisks shows outlier data points. Young N = young normal dogs, Old N = old normal dogs.
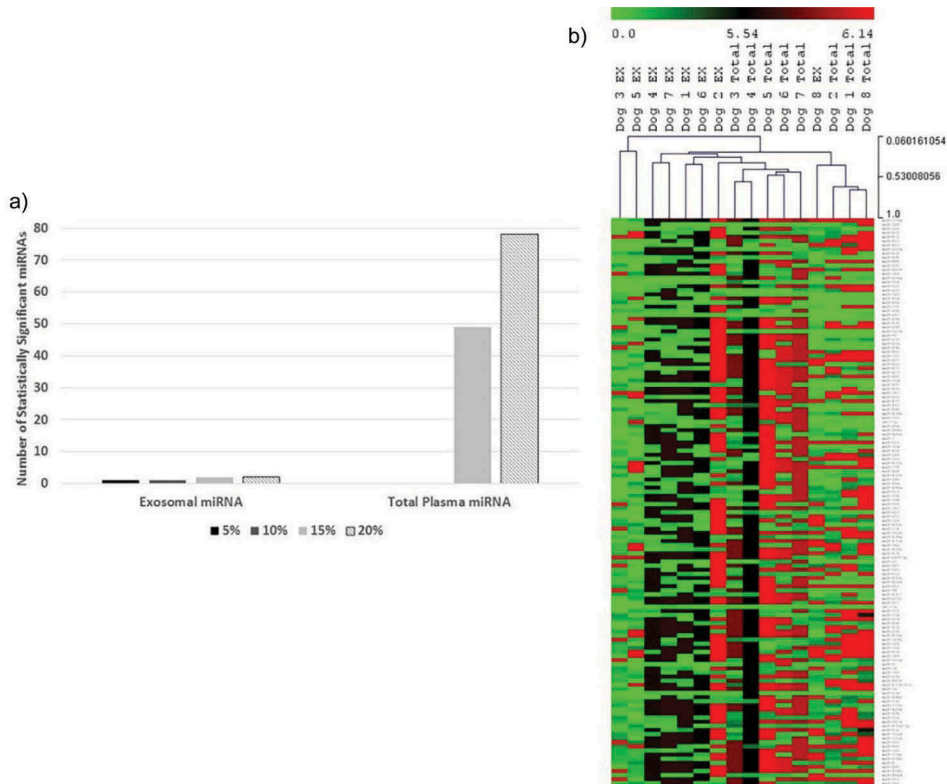

Figure 5. Comparison between ex-miRNA and total plasma miRNA. (a) At least one miRNA (cfa-miR-181c) remained statistically significant for ex-miRNA at a false discovery rate (FDR) as low as 5% when comparing between dogs with and without signs of CHF. The number of significant miRNA dropped from 78 to 0 for total plasma miRNA for a FDR of ≤10%. (b) Hierarchical clustering of plasma exosomal and total plasma miRNA expressions using normalised C_q number for the individual dogs (green = higher expression, red = lower expression). Clustering shows closer association by source of miRNA and not by individual dogs. EX = ex-miRNA; Total = total plasma miRNA.

181c is encoded in the nucleus and assembled in the cytoplasm of the cardiomyocytes and is then translocated into mitochondria to regulate mitochondrial gene expression [22]. In rats, overexpression of miR-181c leads to an increased production of mitochondrial cytochrome C oxidase, which has been associated with mitochondrial dysfunction, increased reactive oxygen species production, increased oxygen consumption in cardiomyocytes, as well as decreased left ventricular ejection fraction [22,23]. In addition, miR-181c contributes to mitochondrial dysfunction and cell death by targeting the Bcl-2 gene, an apoptosis regulator [24,25].

The higher variability in cfa-miR-181c expression observed in older normal dogs may be a result of general cell senesce, mitochondrial dysfunction and oxidative damage with ageing. However, given the significant increase in cfa-miR-181c expression in MMVD-CHF, miR-181c may serve as an important biomarker or therapeutic target in patients at risk for developing CHF.

Plasma exosomal miR-495, which is repressed with age, increases with MMVD-CHF

This ex-miRNA was upregulated with heart disease, particularly in advanced disease with CHF in defiance of its age-related trend downward. Similar to the present observation, Clark *et al.* observed an upregulation of miR-495 not only in young, perinatal hearts but also in diseased hearts in response to stress stimuli [26,27]. Similar to cfa-miR-9, expression of cfa-miR-495 appeared to be age-related in the current study, with a decrease in expression in older healthy animals.

miR-495 overexpression has been shown to stimulate cardiomyocyte DNA synthesis and proliferation [27]. The proliferation-inducing effects of miR-495 would be consistent with cardiac hypertrophy seen in advanced heart diseases with cardiac remodelling. Although speculative, cfa-miR-495 may also serve as a potential biomarker to help monitor progression to active CHF in addition to cfa-miR-181c.

Exosomal miR-599 declines in MMVD compared to age-matched controls

An increase in cfa-miR-599 associated with ageing was observed. Studies have shown that this miRNA can inhibit vascular smooth-muscle cell proliferation and production of collagen I, collagen V and proteoglycan by direct targeting of TGFβ2 [28]. Interestingly, there is a downregulation of cfa-miR-599 in dogs with MMVD when compared to normal older dogs. Given that MMVD is a disease with dysregulation of collagen and matrix proteoglycan production, further study of the involvement of miR-599 in MMVD disease genesis is warranted.

Interaction of miR-9, miR-181c and miR-495

MiRNA target predictions show common gene targets that may be regulated in common by cfa-miR-9, cfa-miR-181c and cfa-miR-495 (Figure 6), suggesting a network that deserves further attention. However, no commonality was found among these three miRNA with cfa-miR-599. There are two common targets between cfa-miR-9, cfa-miR-181c and cfa-miR-495: AGFG1 and FAM126B. AGFG1 has homology to nucleoporins [30], the significance of which relating to CHF or MMVD is unclear at this time. FAM126B was found to be downregulated in atrial tissue for human patients who develop atrial fibrillation after coronary artery bypass graft surgery [31].

Five additional common targets exist between cfa-miR-181c and cfa-miR-miR-495, and 24 additional common targets exist between cfa-miR-495 and cfa-miR-9. Of these common targets shared between cfa-miR-9 and cfa-miR-495, eight of them are associated with cardiac fibrosis, cellular energy production, Ca^{2+} homeostasis or cardiac remodelling. Target genes that are involved in fibrosis include CCDC88A [32], SMURF2 [1] and TRPM7 [33]. SCL8A1 is involved in Ca^{2+} homeostasis in both mitochondria and cardiomyocytes and has been implicated in the development of arrhythmias and heart failure [34]. Target genes involved in cardiomyocyte cell cycling include DYRK1A [35], KLF5 [36] and HIPK [37]. Finally, GRSF1 is important in maintaining
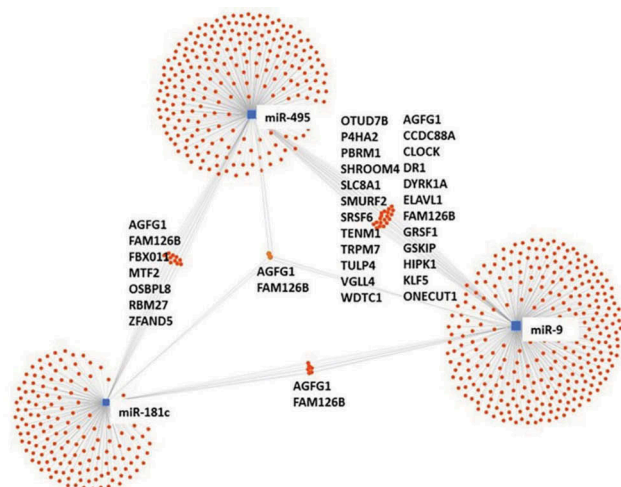

Figure 6. Target interaction network. MiRNA target interaction network for cfa-miR-9, cfa-miR-181c and cfa-miR-495. No interaction can be found with cfa-miR-599 (schematic modified from miRNet.ca) [29].

mitochondrial RNA stability [38]. These common target genes suggest that cfa-miR-9 and cfa-miR-495 have important roles in fibrosis control, cardiomyocyte replication and energetics. The high number of target genes implicated in the regulation of fibrosis is compelling, given that previous studies in canine MMVD valvular tissue showed an increased concentration of collagen I, III, IV and VI and fibronectin in the diseased areas of the valve [39]. In addition, there is an increase in TGFβ1 and 3 expression in these valves [40]. Similarly in humans, upregulation in TGFβ expression has also been implicated [41].

Study limitations

These training data sets yielded candidate circulating ex-miRNA that need to be further verified using a variety of experiments, including target expression in tissues, gain and loss of function in canine cell lines, studies that define the biological activity of exosomes and ex-miRNA on cell lines *in vitro* and verification of high priority candidate ex-miRNA in blood of larger numbers of patients at different stages of the disease. These data represent a vital step forward in advancing ex-miRNA as important biomarkers for non-ischemic heart disease.

Based on the present disease model, two miRNA were found, specifically miR-495 and miR-181c, whose rise in expression level coincides with the observation of CHF. The authors acknowledge that dysregulation of these ex-miRNA may not be unique to CHF secondary to MMVD, but rather may be a signature of canine heart failure which is a consequence of other aetiologies. A separate control group consisting of dogs with CHF secondary to another type of heart disease would be elucidative. It is also acknowledged that in order to establish definitely that exosomal miRNA track the progression from normal valve to MMVD to MMVD-CHF, a longitudinal study following individual dogs is warranted. Given that a high percentage of dogs with left heart enlargement progress to CHF (within 1–2 years), this would be most feasible at this stage.

Despite the small sample sizes in this study, it was possible to detect significant changes in ex-miRNA expression using a FDR as low as 5%. This may relate to the greater genetic homogeneity of the canine species, or the grouping of dogs into strikingly different categories (age, disease and heart failure).

A limitation to the comparison between miRNA from total plasma and plasma exosomes is the use of different sets of dogs (although eight of the dogs were used in *both* studies). However, given that all of these dogs were categorised into disease groups using the same criteria, and each group of dogs is representative of its disease state, the comparison between total plasma and ex-miRNA should therefore remain valid. The present findings highlight that comparison of total plasma miRNA between groups yields numerous false positives, relative to the low false-positive rate of plasma exosome miRNA analysis. While this analysis may be confounded by the poor age matching between normal and diseased dogs, there was no significant difference between the age of the MMVD and MMVD-CHF groups. Therefore, analysis of total plasma miRNA is a relatively inefficient, non-specific method for detection of disease-relevant miRNA.

Based on this study, the source of the circulating miRNA cannot be identified. The ex-miRNA significantly associated with disease state in this study are found in multiple organs (i.e. not just the heart). CHF and even asymptomatic MMVD have systemic effects due to haemodynamic and neurohormonal consequences that affect blood flow to and functions of many organs. Therefore, it is plausible that circulating candidate ex-miRNA may originate outside the heart. This warrants evaluation by comparing miRNA from diseased and normal heart tissue.

Another limitation is the detection limit of RT-qPCR. Therefore, circulating miRNA with low copy numbers may not have been detected or analysed by this study.

Conclusions

Plasma ex-miRNA show great promise as biomarkers for MMVD disease monitoring and may also help elucidate the pathophysiology of the disease and subsequently help devise therapeutic strategies. The present data show that cfa-miR-9, cfa-miR-181c, cfa-miR-495 and cfa-miR-599 expressions not only change with disease progression and development of heart failure, but also exhibit changes as a function of age. Since MMVD in dogs is a disease more commonly seen in older animals, age-related changes in miRNA expression may be contributor. The exact function and effects of these individual miRNA on valvular cells, cardiomyocytes and cardiac fibroblasts will need to be further elucidated using in vitro assays.

MMVD is an example of a companion animal disease model that can enable the study of ex-miRNA at various stages of the natural history of a disease. The use of naturally occurring disease models provide unique insight into the interplay of epigenetics and the environment, predispositions towards heart failure and new molecular targets for MMVD in humans.

Disclosure statement

Funding

References

[1] Hagler MA, Hadley TM, Zhang H, et al. TGF-β signalling and reactive oxygen species drive fibrosis and matrix remodelling in myxomatous mitral valves. Cardiovasc Res. 2013;99:175–184.

[2] Bonow RO, Carabello BA, Chatterjee K, et al. 2008 Focused update incorporated into the ACC/AHA 2006 guidelines for the management of patients with valvular heart disease. JACC. 2008;52:e1–142.

[3] Borgarelli M, Buchanan JW. Historical review, epidemiology and natural history of degenerative mitral valve disease. J Vet Cardiol. 2012;14:93–101.

[4] Ha M, Kim VN. Regulation of microRNA biogenesis. Nat Rev. 2014;15:509–524.

[5] Chen Y, Wakili R, Xiao J, et al. Detailed characterization of microRNA changes in a canine heart failure model: relationship to arrhythmogenic structural remodeling. J Mol Cell Cardiol. 2014;77:113–124.

[6] Zhang Y, Zheng S, Geng Y, et al. MicroRNA profiling of atrial fibrillation in canines: miR-206 modulates intrinsic cardiac autonomic nerve remodeling by regulating SOD1. PLoS One. 2015;10:e0122674.

[7] Li Q, Freeman LM, Rush JE, et al. Expression profiling of circulating microRNAs in canine myxomatous mitral valve disease. In J Mol Sci. 2015;16:14098–14108.

[8] Hulanicka M, Garncarz M, Parzeniecka-Jaworska M, et al. Plasma miRNAs as potential biomarkers of chronic degenerative valvular disease in Dachshunds. BMC Vet Res. 2014;10:205–212.

[9] Andaloussi SE, Mager I, Breakefield XO, et al. Extracellular vesicles: biology and emerging therapeutic opportunities. Nat Rev. 2013;12:347–357.

[10] Barile L, Moccetti T, Marban E, et al. Roles of exosomes in cardioprotection. Eur Heart J. 2016;ehw304.

[11] Atkins C, Bonagura J, Ettinger S, et al. Guidelines for the diagnosis and treatment of canine chronic valvular heart disease. J Vet Intern Med. 2009;23:1142–1150.

[12] Witwer KW, Buzas EI, Bemis LT, et al. Standardization of sample collection, isolation and analysis methods in extracellular vesicle research. J Extracell Vesicles. 2013;2:20360.

[13] Colombo M, Raposo G, Thery C. Biogenesis, secretion, and intercellular interactions of exosomes and other extracellular vesicles. Annu Rev Cell Dev Biol. 2014;30:255–289.

[14] Murray MJ, Raby K, Saini HK, et al. Solid tumors of childhood display specific serum microRNA profiles. Cancer Epidemiol Biomarkers Prev. 2014;24:350–361.

[15] Pritchard CC, Cheng HH, Tewari M. MicroRNA profiling: approaches and considerations. Nat Rev. 2012;13:358–369.

[16] Benjamini Y, Hochberg Y. Controlling the false discovery rate: a practical and powerful approach to multiple testing. J R Stat Soc Soc B. 1995;57:289–300.

[17] Agarwal V, Bell GW, Nam JW, et al. Predicting effective microRNA target sites in mammalian mRNAs. eLife. 2015;4:e05005.

[18] Wong N, Wang X. miRDB: an online resource for microRNA target prediction and functional annotations. Nucleic Acids Res. 2015;43:D146–D152.

[19] Saeed AI, Sharov V, White J, et al. TM4: a free, open-source system for microarray data management and analysis. Biotechniques. 2003;34:374–378.

[20] van der Pol E, Coumans FAW, Grootemaat AE, et al. Particle size distribution of exosomes and microvesicles determined by transmission electron microscopy, flow cytometry, nanoparticle tracking analysis, and resistive pulse sensing. J Thromb Haemost. 2014;12:1182–1192.

[21] Wang L, Ma LK, Fan H, et al. MicroRNA-9 regulates cardiac fibrosis by targeting PDGFR-β in rats. J Physiol Biochem. 2016;72:213–223.

[22] Das S, Ferlito M, Kent OA, et al. Nuclear microRNA regulates the mitochondrial genome in the heart. Circ Res. 2012;110:1596–1603.

[23] Das S, Bedja D, Campbell N, et al. miR-181c regulates the mitochondrial genome, bioenergetics, and propensity for heart failure in vivo. PLoS One. 2014;9:e96820.

[24] Ouyang YB, Lu Y, Yue S, et al. miR-181 targets multiple Bcl-2 family members and influences apoptosis and mitochondrial function in astrocytes. Mitochondrion. 2012;12:213–219.

[25] Wang H, Li J, Chi H, et al. MicroRNA-181c targets Bcl-2 and regulates mitochondrial morphology in myocardial cells. J Cell Mol Med. 2015;19:2084–2097.

[26] Clark AL, Maruyama S, Sano S, et al. miR-410 and miR-495 are dynamically regulated in diverse cardiomyopathies and their inhibition attenuates pathological hypertrophy. PLoS One. 2016;11:e0151515.

[27] Clark AL, Naya FJ. MicroRNAs in the myocyte enhancer factor 2 (MEF2)-regulated Gtl2-Dio3 noncoding RNA locus promote cardiomyocyte proliferation by targeting the transcriptional coactivator Cited2. J Biol Chem. 2015;290:23162–23172.

[28] Xie B, Zhang C, Jiang S. miR-599 inhibits vascular smooth muscle cells proliferation and migration by targeting TGFB2. PLoS One. 2015;10:e0141512.

[29] Fan Y, Siklenka K, Arora SK, et al. miRNet - dissecting miRNA-target interactions and functional associations through network-based visual analysis. Nucl Acids Res. 2016;44:W135–W141.

[30] Fritz CC, Zapp ML, Green MR. A human nucleoporin-like protein that specifically interacts with HIV Rev. Nature. 1995;376:530–533.

[31] Kertai MD, Qi W, Li YJ, et al. Gene signatures of post-operative atrial fibrillation in atrial tissue after coronary artery bypass grafting surgery in patients receiving β-blockers. J Mol Cell Cardiol. 2016;92:109–115.

[32] Hayano S, Takefuji M, Maeda K, et al. Akt-dependent Girdin phosphorylation regulates repair processes after acute myocardial infarction. J Mol Cell Cardiol. 2015;88:55–63.

[33] Xu T, Wu BM, Yao HW, et al. Novel insights into TRPM7 function in fibrotic diseases: a potential therapeutic target. J Cell Physiol. 2015;230:1163–1169.

[34] Khananshvili D. The SLC8 gene family of sodium–calcium exchangers (NCX) – Structure, function, and regulation in health and disease. Mol Aspects Med. 2013;34:220–235.

[35] Hille S, Dierck F, Kuhl C, et al. Dyrk1a regulates the cardiomyocyte cell cycle via D-cyclin-dependent Rb/E2f-signalling. Cardiovasc Res. 2016;110:381–394.

[36] Drosatos K, Pollak NM, Pol CJ, et al. Cardiac myocyte KLF5 regulates Ppara expression and cardiac function. Circ Res. 2016;118:241–253.

[37] Liu X, Xiao J, Zhu H, et al. miR-222 is necessary for exercise-induced cardiac growth and protects against pathological cardiac remodeling. Cell Metab. 2015;21:584–595.

[38] Antonicka H, Sasarman F, Nishimura T. The mitochondrial RNA-binding protein GRSF1 localizes to RNA granules and is required for posttranscriptional mitochondrial gene expression. Cell Metab. 2013;17:386–398.

[39] Aupperle H, Marz I, Thielebein J. Immunohistochemical characterization of the extracellular matrix in normal mitral valves and in chronic valve disease (endocardiosis) in dogs. Res Vet Sci. 2009;87:277–283.

[40] Aupperle H, Marz I, Thielebein J, et al. Expression of transforming growth factor-β1, -β2 and -β3 in normal and diseased canine mitral valves. J Comp Path. 2008;139:97–107.

[41] Geirsson A, Singh M, Ali R, et al. Modulation of transforming growth factor-β signaling and extracellular matrix production in myxomatous mitral valves by angiotensin II receptor blockers. Circulation. 2012;126 (suppl 1):S189–S197.